Generation and structural properties of internal waves in Hood Canal

Drew Vagen

School of Oceanography

University of Washington

Abstract

Internal waves were first reported by Vilhelm Bjerknes as the phenomenon called “dead water”, and can now be observed all over the world. In Hood Canal, a fjord in the southwestern portion of Puget Sound, internal waves can be observed propagating along the channel. In this study, Seagliders are used to collect profiles of temperature, salinity, and pressure which are used to calculate vertical wave modes and vertical water displacement. The study looks at the structure of internal waves seen in Hood Canal and discusses their mechanisms for generation.

Introduction

Internal waves were first presented by Vilhelm Bjerknes as the phenomenon called “dead water”. Bjerknes remarked that in the case of a layer of freshwater resting on top of a layer of salt water, a ship will not only produce the ordinary visible waves at the air-sea boundary, but will also generate invisible waves in the boundary between freshwater and salt water. The ships resistance to forward movement was due to the work done in generating these invisible waves, resulting in “dead water” (Gill, 1982). Internal waves explain this phenomenon, and they can be observed all around the world.

Hood Canal is a long narrow fjord constituting the southwestern portion of the Puget Sound system of inland waters in Washington State. Freshwater input into the canal comes from several rivers while the influx of seawater comes from the ocean via Admiralty Inlet and the Strait of Juan de Fuca. There is a shallow sill at the northern end of the canal, which, combined, with the shape of the canal, limits the circulation and mixing of water throughout the fjord. Because of the limited circulation and mixing, Hood Canal is predisposed to low oxygen concentrations and hypoxic conditions.

We expect to see internal waves as part Hood Canal’s natural variability. Internal waves arise from density perturbations within a stratified fluid, and typically have much lower frequencies and higher amplitudes than surface waves. At large scales, internal waves are influenced both by the rotation of the Earth as well as by the stratification of the medium. The generation of internal waves in

Hood Canal could be attributed to wind stress forcing at the surface, tidal currents, or a combination of both.

Wind stress is the shear stress exerted by the wind on the surface of large bodies of water such as Hood Canal. The air blowing parallel to the surface instigates a downward transfer of momentum from the air to the water that ultimately generates a drift current underneath. From this current and the energy changes associated with it internal waves can form.

The dominant currents in Hood Canal are associated with tidal sea level changes. A semi-diurnal structure produces two highs in sea level, with amplitudes up to ~4 meters, and two lows per day each, along with intervening strong tidal currents. From the forcing of the surface tide in the stratified waters of Hood Canal over topography an internal tide is formed. Internal tides are internal waves that oscillate at tidal frequencies, and play a large role in dissipating tidal energy and mixing of the water column.

The study utilizes two Seagliders, autonomous profiling floats that can continuously dive and climb while recording and transmitting data of interest such as depth, temperature, and salinity (Eriksen et al., 2001). The Seagliders profile vertically while moving towards pre-programmed locations to create a sawtooth pattern transect. Seagliders can be piloted remotely, and transmit through the satellite Iridium network back to the University of Washington. This study used two Seagliders to study the generation of internal waves and their properties.

This study sets out to investigate the generation method of internal waves in Hood Canal and the structural properties of internal waves and the water column. The generation and structure of internal waves have not previously been studied in Hood Canal, and it is unclear weather or not the internal waves are tidally driven. It is important to determine the internal wave generation and structure of Hood Canal because it is a prominent source of density displacement within the fjord, which in turn influences mixing throughout the water column.

Methods

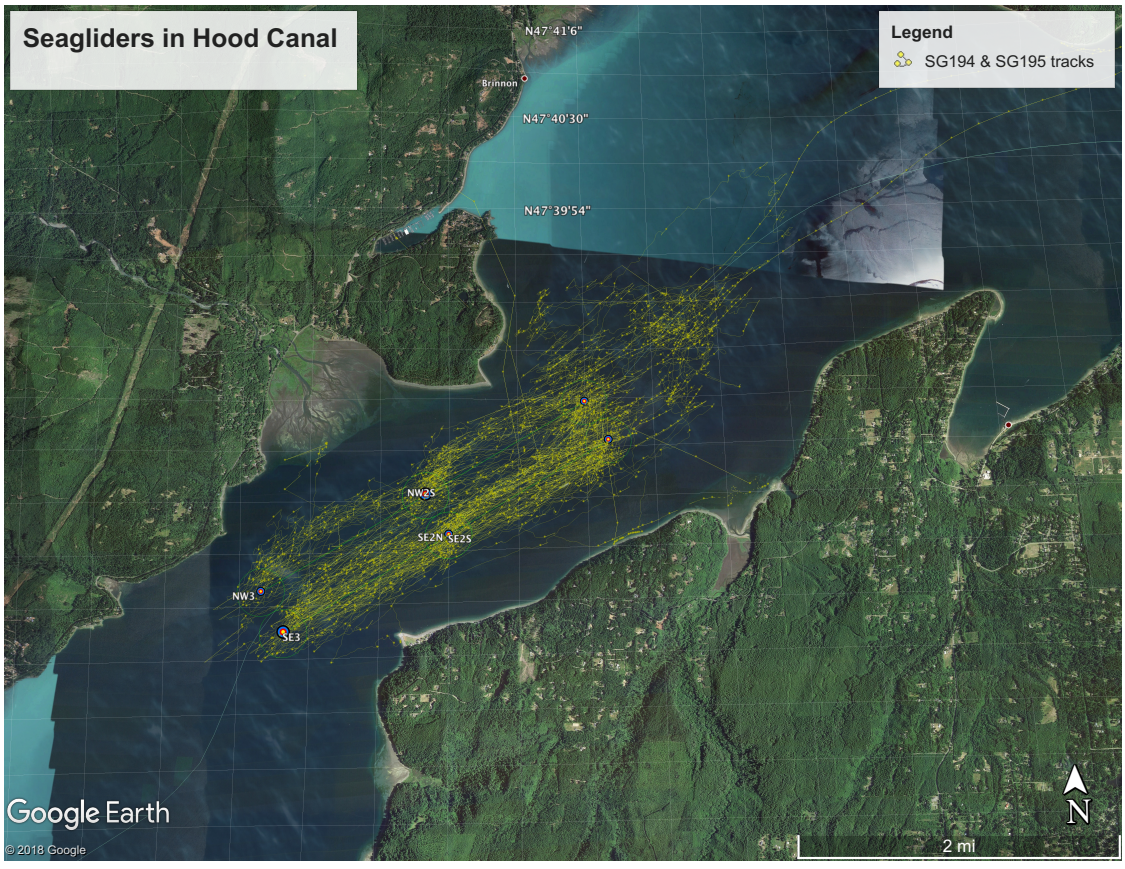

Figure 1: Seaglider profiling tracks for sg194 and sg195

Two Seagliders were deployed on January 31, 2018 in the northern end of Hood Canal at 47.644° N and 122.87° W. The Seagliders ran continuous profiling transects until March 2, 2018 when they were recovered (Figure 1). The Seagliders were programmed to specific coordinates, and moved from surface to depth creating a saw tooth pattern of continuous profiling. The Seagliders transmitted the collected data, which included: latitude/longitude, temperature, salinity, pressure, density, and dissolved oxygen, through satellite Iridium communication every time they were at the surface to the facilities at the University of Washington. Once all of the data had been collected, it was processed into a Matlab-readable file.

The first step of data analysis was to calculate depth into bin-averaged values, which gridded the data onto a uniform depth grid. The bin depths were set to a scale so that a bin-averaged measurement was created every two meters from surface to 40 meters depth, then every 5 meters from 40 up to 160 meters depth, and then every 10 meters deeper than 160 until 200 meters depth. From these bin-averaged values the standard seawater routines were used in matlab to calculate pressure, potential density, and other variables of interest.

To examine how density surfaces fluctuated with time, a contour plot was drawn for varying potential density surfaces with depth (Figure 2). Potential density was calculated from salinity, temperature, and pressure profiles for each Seaglider dive. The calculated potential density was then separated into specific isopycnals and contoured against time.

To compare the potential density fluctuations with the Hood Canal tides, predictions of tidal high and low available from the National Oceanographic and

Atmospheric Administration (NOAA) at their Pleasant Harbor station were used from the same dates that the Seagliders were deployed. These tidal extrema were interpolated to the same values between high and low tide and gridded to the same hourly scale as the isopycnal data. The tidal data was then plotted on top of the isopycnal fluctuations.

Isopycnal vertical displacements were calculated from the bin-averaged potential density time series. Using the formula:

$$\eta(z,t) = \frac{\sigma(z,t) - \bar{\sigma}(z)}{-\frac{\partial \sigma}{\partial z}}$$

where $\sigma(z,t)$ is the high pass filtered potential density anomaly at height z and time t, $\bar{\sigma}$ is the time-averaged potential density anomaly at height z, and $\frac{\partial \sigma}{\partial z}$ is its vertical derivative. Once the displacement was calculated for every depth, the values were low-pass filtered using the triangular function mentioned earlier for smoothing purposes. The original displacement values were then subtracted from the low-pass filtered values to get the actual displacement in meters for each depth level. The calculated displacements were then contoured against time to show the temporal variability.

To investigate the structure of the internal tide, the vertical normal modes for long waves were calculated. The time-mean buoyancy frequency profile N(z) was first calculated using the standard seawater routine for each bin depth. The barotropic mode and 29 baroclinic modes were calculated by solving the vertical structure equation:

$$c^2 G''(z) + \langle N(z) \rangle^2 G(z) = 0$$

which was subject to vanishing vertical displacement at the flat bottom and allowance of a free sea surface. The constant c is the kelvin wave speed for each mode. This showed their respective horizontal velocities G'(z) and vertical displacements G(z). Hourly vertical displacement profiles were fit by a sum of vertical displacement normal modes.

Lastly, the potential energy per unit horizontal mass was calculated for the internal wave mode spectra. The PE was found by integrating over the water column:

$$PE = \frac{1}{2}\sum_{m=1}^{m=\infty} \langle \beta_m^2(x,y,t) c_m^2 \rangle$$

where β_m(x, y, t) is the projection coefficient of a given vertical displacement profile on a certain modal shape.

Results

For the investigation, 656 dives were analyzed from Seaglider 195 (sg195). Profiles from Seaglider 194 (sg194) were not analyzed due to evident pressure sensor drift.

Sg195 ran continuous tracks between 47.65N and 47.61N within a relatively straight and deep section of Hood Canal southwest of Dabob Bay and in between Quatsap Point and Hood Point. From measurements along the sg195 tracks, density profiles were produced and then contoured in depth versus time (Figure 2). The contour plot shows various isopycnals and their variations in time, producing a slightly downward trend in the mid-depth range. Density variation near the surface

was quite energetic, likely due to lateral salinity variations supplied by variable freshwater sources within Hood Canal. Density varies little so that influence of vertical displacement from a weakly stratified deep mean profile produces noisy results.

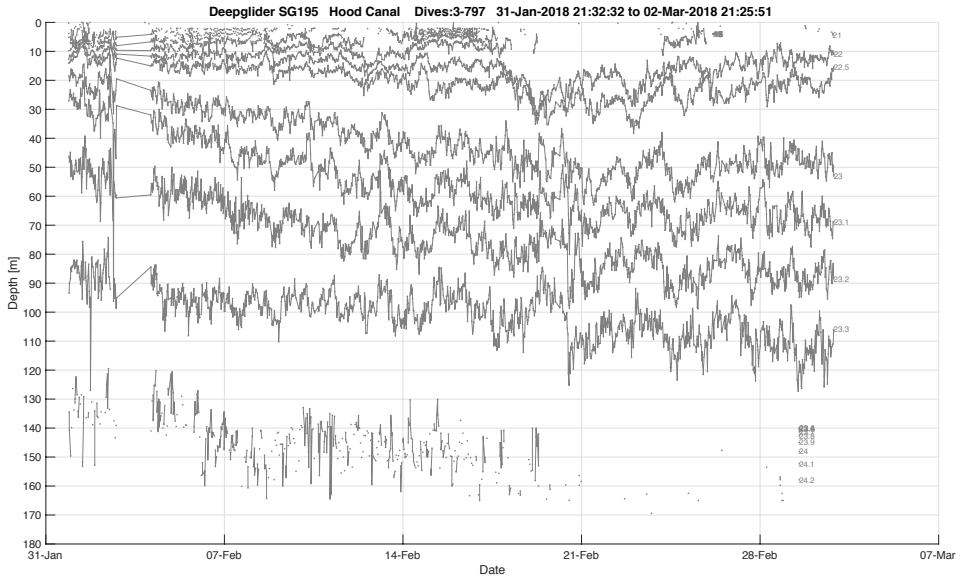

Figure 2: Progression of isopycnals over time. Density surfaces were extracted at many different depths and contoured against time, showing the temporal and spatial variability of the isopycnals.

From the salinity and temperature profiles a bin-averaged buoyancy frequency N(z) was calculated (Figure 3). This is the angular frequency at which a vertically displaced parcel will oscillate within a stratified fluid. The average N(z) profile shows a strong peak associated with the transition from relatively fresh near surface waters to relatively saline deep waters. The peak averaged N(z) value was 0.049 s^{-1} while at depth values were stable around 0.003 s^{-1}.

From the average temperature and salinity profiles obtained by sg195, the vertical structure equation for long waves in a channel of uniform depth was solved. The barotropic mode explains how current fluctuations at the mean density would

appear in the absence of stratification while the baroclinic modes arise from stratification of the water column and show natural internal normal modes of variability both in the current (blue curves, Figure 3) and in vertical displacements (red curves, Figure 3). The horizontal Kelvin wave speed was calculated for each mode, with the first baroclinic mode showing the highest speed at 0.5314 m/s.

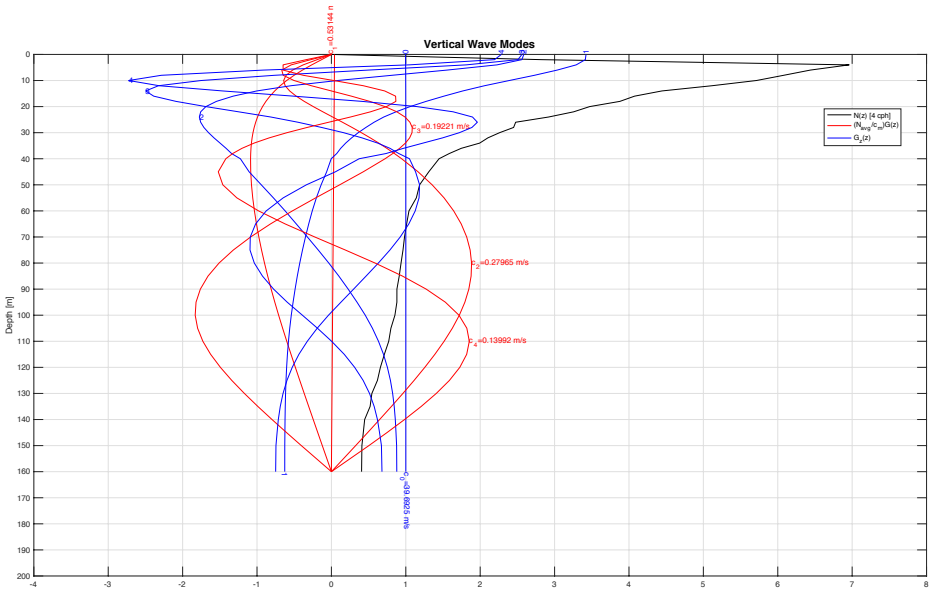

Figure 3: The barotropic and first five baroclinic modes were calculated and plotted to show the modal shape and horizontal kelvin wave speed. The black curve is the bin-averaged buoyancy frequency, blue curves are calculated wave mode current velocities, and the red curves are calculated vertical mode displacement.

Using density profiles, the vertical displacement (η) was calculated for each bin depth on an hourly scale (Figure 4). It was important to filter the calculations to get rid of big trends that arise due to wind stress on Hood Canal. The filtering removed low-frequency trends that were not due to internal waves. The time series had a maximum positive displacement of 16.90 meters, which occurred at a depth of 125 meters.

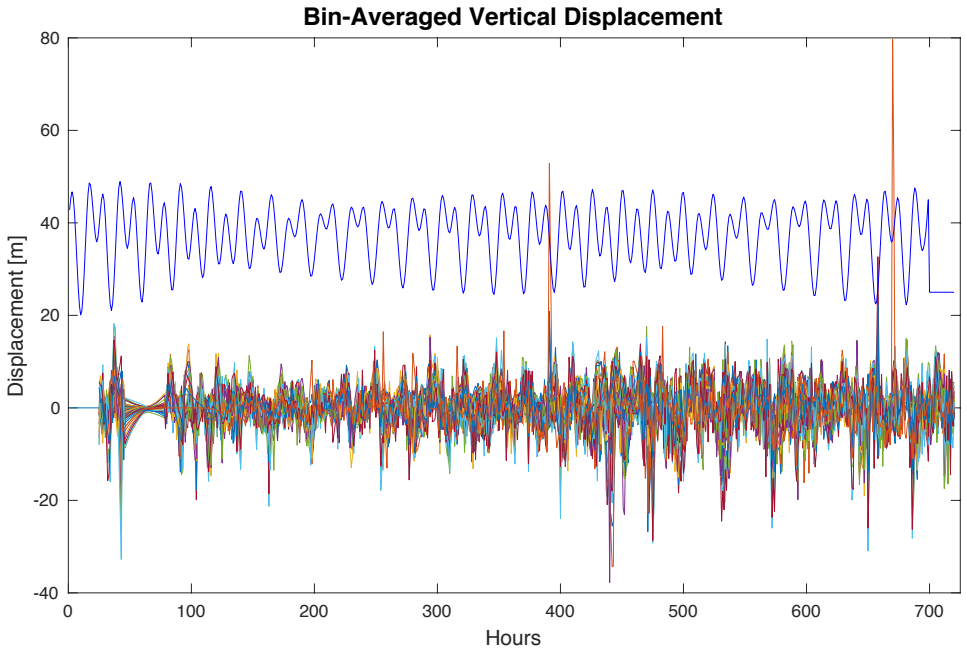

Figure 4: Calculated vertical displacements for every bin depth (colored lines) was plotted against time to show the variability in vertical displacement. The tide (blue line) was scaled and plotted above the vertical displacements to show how the tidal peaks matched with vertical displacement peaks.

Since the vertical displacements for every depth had already been calculated, a calculation was done to fit vertical wave modes to the displacements (Figure 5, top). The vertical wave modes were also fitted to profiles of the buoyancy frequency times displacement ($N * \eta$) (Figure 5, bottom). The fit showed consistent matching of η and $N * \eta$ with the vertical wave mode structures.

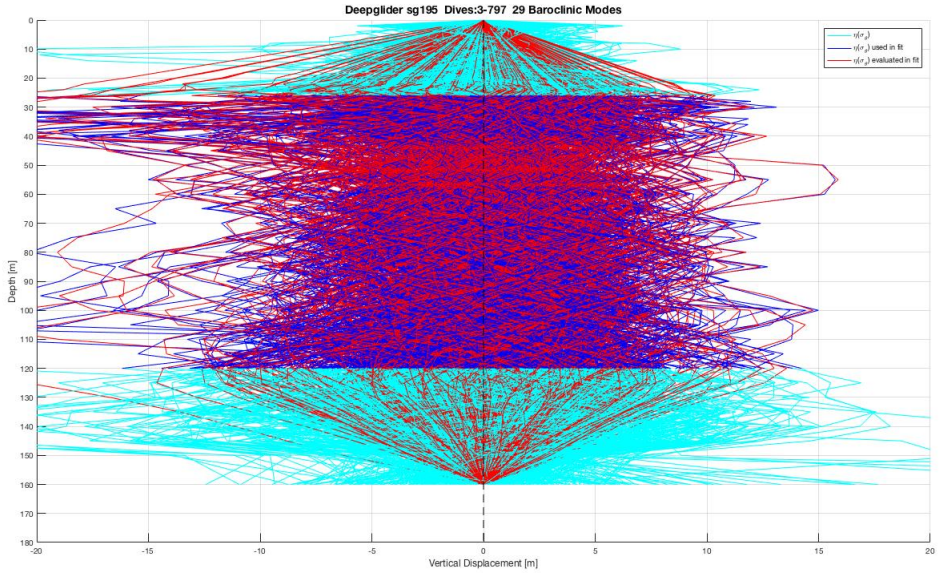

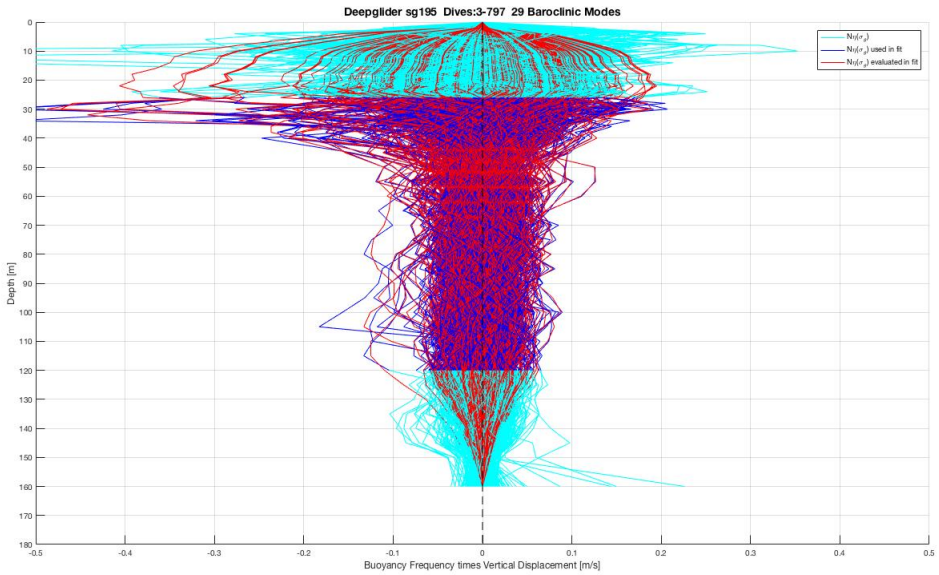

Figure 5: Top figure shows the vertical displacement in cyan, with the 29 modal shapes in red and the calculated modal fit in blue. Bottom figure shows the vertical displacement times the buoyancy frequency in cyan, with the 29 modal shapes in red and the calculated modal fit in blue.

To show temporal stratification of profiles of displacement throughout the water column, a mesh plot was made contouring the water column displacement gainst depth and time (Figure 6, top). This 3D visualization showed that displacement affected the whole water column similarly, as patterns of displacement can be seen across all depths. A simple contour plot was also created to show displacement through the water column against time (Figure 6, bottom). The banded structure can be seen across all depths, varying in time, which also implies that vertical displacement is affecting the whole water column similarly.

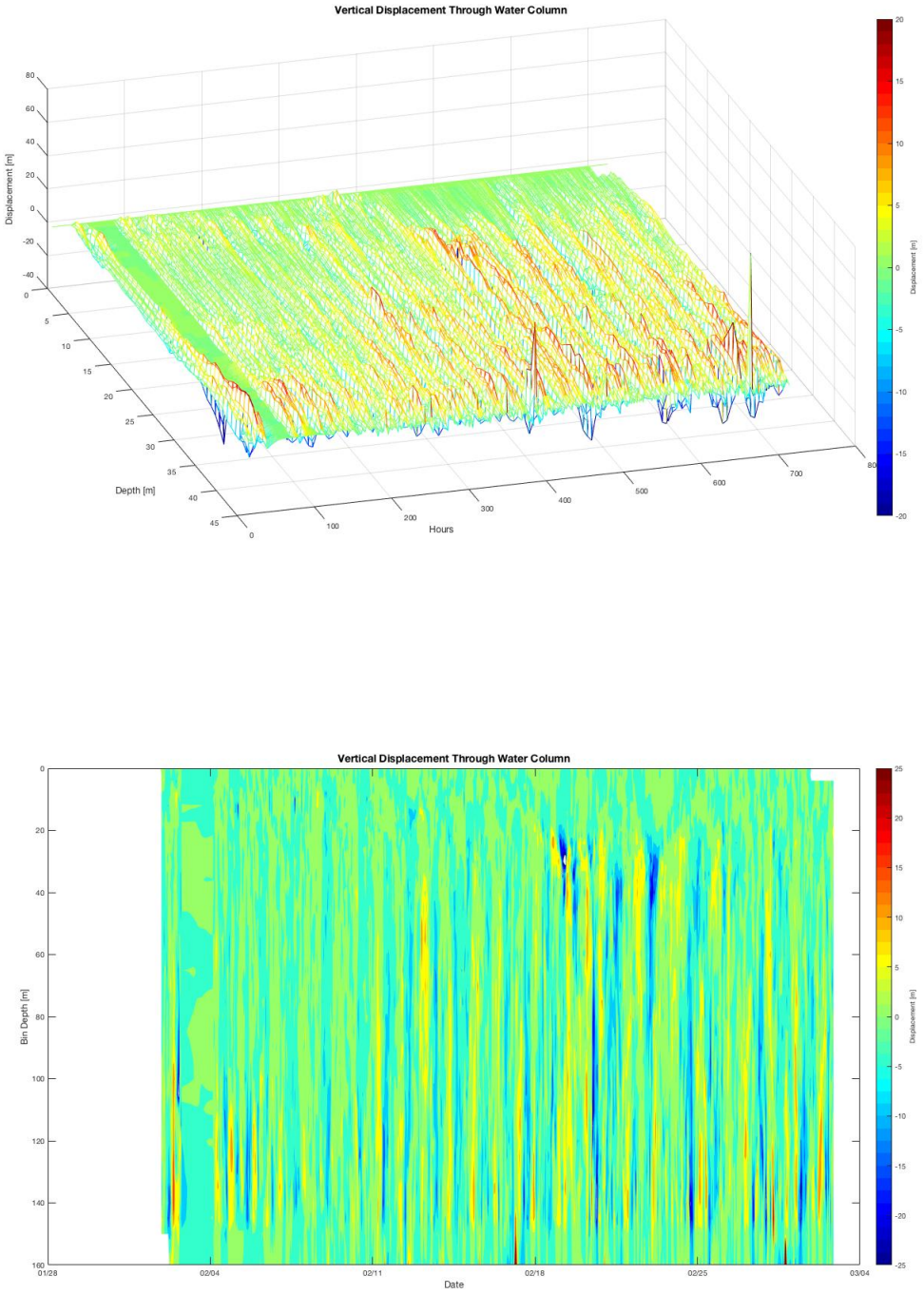

Figure 6: Top figure shows the displacement of the water column against time in a 3D format. The bottom figure shows the contoured displacement through the water column against depth.

A final calculation was done to look at the potential energy per mass spectrum produced by the wave modes (Figure 7). The potential energy per unit mass of waves in a stratified fluid is half the square of the product of buoyancy

frequency N(z) with vertical displacement η. The spectrum varies nearly inversely to the square of modal number over much of the range considered (baroclinic modes 1 through 29).

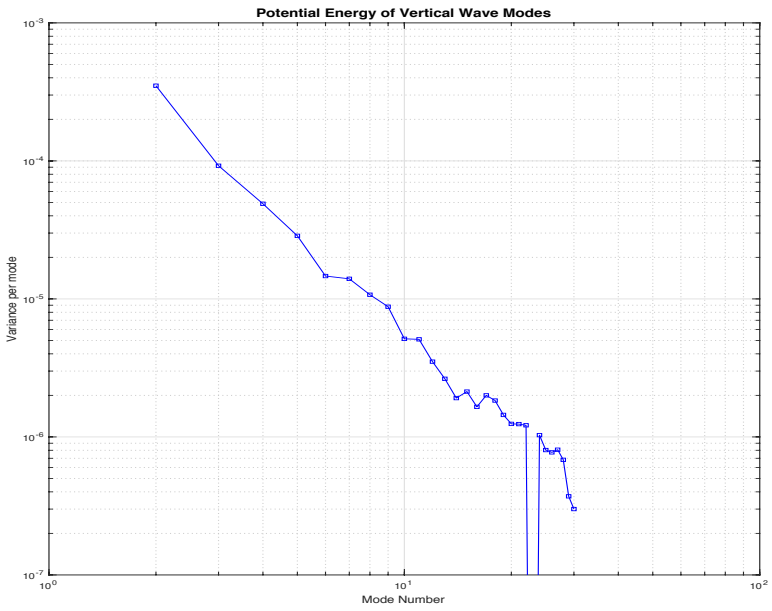

Figure 7: The variance per mode is plotted for each wave mode number. There is a present forcing on a m^{-2} scale.

Discussion

The density perturbations seen in the data arise from vertical movement in the surface of background density of the water. The generation of this vertical movement could be explained by wind stress forcing on the surface. As stated in *Eriksen 1988,* the near-inertial part of the internal wave spectrum is hypothesized to be dominated by the response to wind forcing and can be generated quite efficiently by sharp changes in wind stress. The potential energy spectrum that was derived from the vertical wave modes showed a dependence on an m^{-2} scale, which is what was similarly found in *Eriksen 1988*.

Another possibility for the generation of the internal waves seen could be due to the evolution from the internal tide, which arises through density perturbations from flow over topography. When plotting vertical wave mode displacement against the tidal displacement it seems that baroclinic modes two and four are somewhat tidally dependent and are in phase with each other in certain sections of the time series. It is also shown that the vertical displacement of the water column is very uniform in that positive and negative displacements in time are seen continually throughout the whole water column. This suggests that the disturbances are tidally driven.

Conclusion

The generation of internal waves in Hood Canal is most likely explained by tidal forcing. While there are some wind driven elements to the internal waves observed, this is most likely due to strong surface wind stress within Hood Canal. The more likely explanation for internal wave generation in Hood Canal comes from the tides. The tidal fluctuations in Hood Canal produce strong currents, which likely flow over topography and produce a hydraulic jump causing internal wave generation. The vertical displacement seen in Hood Canal oscillates at a near-tidal frequency, suggesting that the semi-diurnal tide plays a major role in directing internal waves. The m^{-2} scale seen in the potential energy spectrum also shows similarity in the wave mode spectrum that could account for the generation of these waves through forcing in the bottom boundary layer. Forcing in the bottom boundary layer over topography could produce vertical forcing, resulting in

displacement and internal wave generation. We have not yet identified the real source of the internal wave generation, so more observation and modeling is necessary to fully understand the structure and generation of the internal waves in Hood Canal.

Works Cited:

Eriksen, C.c., et al. “Seaglider: a Long-Range Autonomous Underwater Vehicle for Oceanographic Research.” *IEEE Journal of Oceanic Engineering*, vol. 26, no. 4, 2001, pp. 424–436., doi:10.1109/48.972073.

Eriksen, Charles C. “On Wind Forcing and Observed Oceanic Wave Number Spectrum.” *Journal of Geophysical Research*, vol. 93, no. C5, 15 May 1988.

“Atmosphere-Ocean Dynamics.” *Atmosphere-Ocean Dynamics*, by Adrian E Gill, Academic Press, 1982, pp. 123–124.